Title

Directing the Rate-Enhancement for Hydronium Ion Catalyzed Dehydration via Organization of Alkanols in Nanoscopic Confinements

Journal

Angewandte Chemie International Edition, 60(5)

ISSN

1433-7851

Authors

Shetty, Manish
Wang, Huamin
Chen, Feng
et al.

Publication Date

2021-02-01

DOI

10.1002/anie.202009835

Peer reviewed

How to cite: *Angew. Chem. Int. Ed.* **2021**, *60*, 2304–2311
International Edition: doi.org/10.1002/anie.202009835
German Edition: doi.org/10.1002/ange.202009835

Heterogeneous Catalysis

Directing the Rate-Enhancement for Hydronium Ion Catalyzed Dehydration via Organization of Alkanols in Nanoscopic Confinements

Manish Shetty, Huamin Wang, Feng Chen, Nicholas Jaegers, Yue Liu, Donald M. Camaioni, Oliver Y. Gutiérrez, and Johannes A. Lercher**

Abstract: *Alkanol dehydration rates catalyzed by hydronium ions are enhanced by the dimensions of steric confinements of zeolite pores as well as by intraporous intermolecular interactions with other alkanols. The higher rates with zeolite MFI having pores smaller than those of zeolite BEA for dehydration of secondary alkanols, 3-heptanol and 2-methyl-3-hexanol, is caused by the lower activation enthalpy in the tighter confinements of MFI that offsets a less positive activation entropy. The higher activity in BEA than in MFI for dehydration of a tertiary alkanol, 2-methyl-2-hexanol, is primarily attributed to the reduction of the activation enthalpy by stabilizing intraporous interactions of the C_β-H transition state with surrounding alcohol molecules. Overall, we show that the positive impact of zeolite confinements results from the stabilization of transition state provided by the confinement and intermolecular interaction of alkanols with the transition state, which is impacted by both the size of confinements and the structure of alkanols in the E1 pathway of dehydration.*

Introduction

Molecular-sized zeolite confinements enhance reaction rates for a wide range of organic transformations.[1] These rate enhancements for active sites within these microenvironments are accompanied by increased complexity at the molecular level that makes understanding the kinetics difficult.[2] Multiple factors influence the activity and selectivity in these environments, as both the adsorbed intermediates and transitions states are influenced by the confinement, often having convoluted effects.[3]

The effects of confinements on adsorption and stabilization of intermediates at gas-solid interfaces have been studied in detail.[1a,b,3,4] Extrapolation of understanding from the gas phase to the condensed phase is challenging, because the organization of the condensed phase in the pores modifies the nature of active sites, the interaction of reaction intermediates with the active sites, and the reaction pathway.[5] In the presence of water, hydrated hydronium ions form. These ions induce a lower standard free energy of activation for cyclohexanol dehydration than unconfined hydronium ions.[5c] Confinements like those in MFI stabilize the transition state (TS) by van der Waals contacts between the TS and the zeolite pores, which in turn leads to a low activation enthalpy that compensates for the lower activation entropy, than wider BEA pores.[5d] Stabilization of the acidic proton relative to positively charged TSs dramatically impacts the rates of acid-catalyzed reactions of hydroxy-containing compounds.[6]

The organization of the solvent and reacting substrate greatly influence the activity of active sites in nanoscopic confinements through enthalpic and entropic stabilization of intermediates and TSs.[7] The intraporous intermolecular interactions including hydrogen bonding of the ground states, reactive intermediates, TSs and surface functionalities including defects (silanol nests) inside zeolite pores create extended structures around active sites and reactive species.[6,7] The free energies of the reactive species and elementary reaction steps are affected by the reorganization of the intraporous environment to accommodate reactive intermediates and TSs.[6–8] Thus, understanding the influence of molecular structure on the organization of substrates, pore environments, and kinetic parameters is crucial for advancing catalyst design and discovery.

Alcohols with a substantial diversity of molecular structures are key intermediates in the valorization of biomass to fuels and chemicals. Therefore, the question arises, how catalysts need to be designed to convert the complex feedstock with balanced rates. On tungstated zirconia, substituted hexanols (secondary and tertiary) and alcohols with methyl branching on the β-carbon exhibit higher reaction rates and lower activation energies than linear alcohols.[9] Considering that zeolites provide higher rates than macroporous solid acids such as tungstated zirconia,[5c,d] we decided to address the impact of size and structure on the condensed phase dehydration of alcohols.

[*] Dr. M. Shetty, Dr. H. Wang, Dr. F. Chen, N. Jaegers, Dr. D. M. Camaioni, Dr. O. Y. Gutiérrez, Prof. J. A. Lercher
Institute of Integrated Catalysis, Pacific Northwest National Laboratory (PNNL)
P.O. Box 999, Richland, WA 99352 (USA)
E-mail: huamin.wang@pnnl.gov
Johannes.lercher@pnnl.gov
Dr. Y. Liu, Prof. J. A. Lercher
Department of Chemistry and Catalysis Research Center, Technical University München
Lichtenbergstrasse 4, 85747 München (Germany)
Supporting information and the ORCID identification number(s) for the author(s) of this article can be found under: https://doi.org/10.1002/anie.202009835.

In this work, we used thermochemical and kinetic measurements, and isotope labeling to quantitatively investigate the reaction pathway and kinetics of C_7 alkanol dehydration. We investigated alkanols with a linear aliphatic chain (3-heptanol) and methyl substitution at α and β-carbon (2-methyl-2-heptanol and 2-methyl-3-hexanol) that effectively mediate the organization of the substrates in the pore and the stabilization of the elimination TS in confined pores in zeolite. The hydronium ions in zeolites lead to lower standard free energy barriers than hydronium ions in aqueous solutions, but both the activation enthalpy and entropy and the reaction pathways inside zeolite pores are affected by the substrate structure and the stabilization of TS within the intraporous zeolite environment.

Results and Discussion

Dehydration of alkanols by unconfined hydronium ions in water

We first consider the dehydration of 3-heptanol, 2-methyl-3-hexanol, and 2-methyl-2-hexanol in aqueous solutions. Phosphoric acid was used to provide unconfined hydronium ions in water. The initial rates of olefin formation are normalized to the concentration of hydronium ions after corrections for temperature, the dissociation equilibrium (pK_a) of phosphoric acid, and the association equilibrium of the alcohol with the hydronium ions in solution (Section S.1.3). The olefin formation rates show fractional positive orders (0.46 ± 0.14, 0.63 ± 0.06 and 0.75 ± 0.03 for 3-heptanol, 2-methyl-3-hexanol and 2-methyl-2-hexanol at 443, 423 and 363 K, respectively) with varying concentration of hydronium ions in solution (Figure S7). We note that the association of alcohols to hydronium ions in solutions (determined from the regression of olefin formation rates at two different concentrations, Figure S5) is nearly thermoneutral ($\Delta H_{l,a}^{o}$ between -1.2 to $-6.2\ kJ\,mol^{-1}$) and leads to a gain in entropy ($\Delta S_{l,a}^{o}$ between 31.6–42.7 $J\,mol^{-1}\,K^{-1}$). The entropy gain is hypothesized to be caused by disruption of the hydrogen bonding network of the hydronium ion due to the association with alcohol.

The olefin formation rates increased marginally from 3-heptanol to 2-methyl-3-hexanol with the branching at β-carbon, along with a large increase from 2-methyl-3-hexanol to 2-methyl-2-hexanol with the origin of branching shifting from β to α-carbon (Figure 1). The apparent activation barriers for the dehydration of 3-heptanol, 2-methyl-3-hexanol, and 2-methyl-2-hexanol decreased from 162 ± 4 to 154 ± 7, and $142 \pm 2\ kJ\,mol^{-1}$, respectively (Figure 1). The apparent activation barriers decreased with increasing stability of the carbenium ions following the C–O bond cleavage step in an E1-elimination pathway from 3-heptanol to 2-methyl-2-hexanol.

Adsorption of alkanols inside zeolite pores

Next, we determine the microenvironment in the pores of zeolites, used for the alkanol dehydration in aqueous solutions. Alkanol adsorption isotherms were first measured and alkanol to BAS ratios were estimated at 298 K. Then, the alkanol to BAS ratios were extrapolated to reaction temperatures to investigate the pore environment under reaction conditions. The water adsorption inside zeolite pores under high water chemical potentials used here, are associated with hydrated hydronium ions.[10] For example, Eckstein et al., reported hydronium ion cluster size of 8 ± 1 H_2O/BAS inside MFI pores.[10] We hypothesize the size of hydronium ion clusters to be slightly larger in BEA pores.

Adsorption isotherms of alkanols on HMFI and HBEA zeolites (henceforth referred as MFI and BEA, respectively) from binary alkanol-water mixtures ($\approx$0.005–0.1 M) were

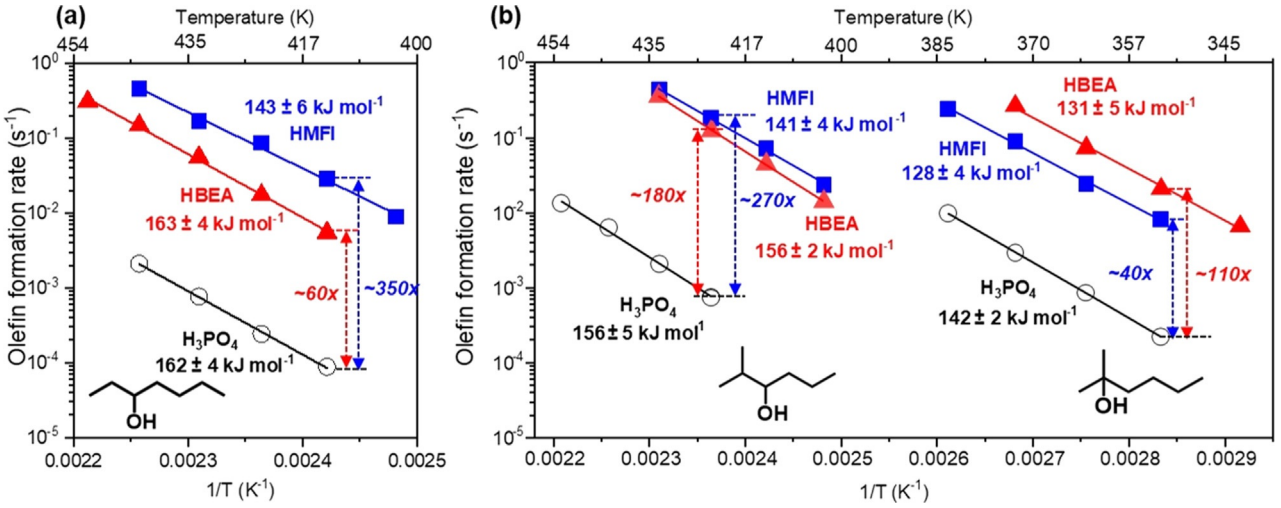

Figure 1. Olefin formation rates ($mol_{alcohol}\,mol_{acid\ sites}^{-1}\,s^{-1}$) and activation energies for dehydration of alkanols; a) 3-heptanol and b) 2-methyl-3-hexanol and 2-methyl-2-hexanol. Reaction conditions: Reactor was pressurized with 40 bar H_2 at ambient temperature and stirred vigorously at 700 r.p.m. Concentration of around 0.2–0.3 M based on density of water at room temperature. The rates were determined from the formation of olefin after the set temperature was reached. Turnover frequencies are determined as olefin formation rates ($mol\,L^{-1}\,s^{-1}$) normalized to the concentration of hydronium ions (H_3PO_4) or total BAS (zeolite). The concentration of hydronium ions in water depends on temperature and alcohol concentration. Activation energies are determined from Arrhenius plots (Supporting Information, Table S2).

Table 1: Adsorption parameters for alcohol uptake into the two zeolites denoted by BEA and MFI at 298 K and reaction conditions (433 K for 3-heptanol and 2-methyl-3-hexanol and 373 K for 2-methyl-2-hexanol).[a]

Substrate	$K_{ads}°$		$\Delta H_{ads}°$ [kJ mol^{-1}]		$\Delta S_{ads}°$ [J mol^{-1} K^{-1}]		q_{max} [mmol g^{-1}]				Θ[c]		Alkanol/BAS[d]	
							298 K		Reaction conditions[b]					
	MFI	BEA	MFI	BEA	MFI	BEA	MFI	BEA	MFI	BEA	MFI	BEA	MFI	BEA
3-heptanol	833 (28)	233 (17)	−27	−21	−36	−24	1.08	1.51	0.62	0.90	0.74–0.87	0.62–0.80	1.47	4.31
2-methyl-3-hexanol	331 (16)	221 (20)	−24	−19	−31	−19	1.02	1.64	0.57	1.06	0.62–0.80	0.67–0.83	1.24	5.27
2-methyl-2-hexanol	246 (41)	199 (43)	−22	−19	−28	−21	0.95	1.77	0.66	1.15	0.80–0.91	0.81–0.91	1.64	6.27

[a] Adsorption constants determined from the slope of the linearized Langmuir isotherm. Adsorption constants reported at 298 K. The numbers in brackets correspond to adsorption constants extrapolated to reaction conditions from 298 K. [b] q_{max} extrapolated from thermal expansion reaction conditions from 298 K. [c] Θ refers to fraction of the total uptake at concentration range of 0.10–0.25 M at the same temperature for $K_{ads}°$ and q_{max} for the alkanols. [d] Alkanol/BAS estimated at 0.25 M concentration.

measured between 280 and 313 K to investigate the environment inside the zeolite pores (Figure S9 and Section S.1.6). The physicochemical properties are compiled in Supplementary Table S1 and Figures S1–S4. By fitting Langmuir adsorption isotherms to the uptakes, the equilibrium constants ($K_{ads}°$) and saturation uptakes (q_{max}) were determined (Table 1). At 298 K, the ratio of saturation uptake of alcohol to the BAS (Alkanol/BAS) were determined to be ≈2.9, 2.7 and 2.5 in MFI, and 8.9, 9.6 and 10.4 on BEA, for 3-heptanol, 2-methyl-3-hexanol and 2-methyl-2-hexanol, respectively (Table 1). Adsorption enthalpies ($\Delta H_{ads}°$) were determined from the Van't Hoff plot of $K_{ads}°$. The $K_{ads}°$ of alcohol is lower with BEA than with MFI pores. The $\Delta H_{ads}°$ and $\Delta S_{ads}°$ were lower with MFI than with BEA because of the stronger dispersive interactions of the alcohols with the narrower pore of MFI. In both zeolites, the $K_{ads}°$ of the alcohol inside the pores decreased as its branching increased, but to a larger extent in MFI than in BEA. This is attributed to the less ideal fit and the beginning of repulsive interactions of the branched alkanes analogous to similar observations with alkanes.[11] This phenomenon is well documented by the higher $\Delta H_{ads}°$ from 3-heptanol to 2-methyl-2-hexanol. In the larger BEA pore, the lower interaction of alcohol molecules with the larger BEA pore leads to minimal changes with the alcohol structure. Any variations in $\Delta H_{ads}°$ were, however, compensated for by a variation in $\Delta S_{ads}°$ showing a perfect compensation behavior for all alcohols and zeolites studied. The negative $\Delta S_{ads}°$ contributes to the lowering of $K_{ads}°$ at higher temperatures.

The maximum uptake of alcohols (q_{max}) did not vary markedly for the same zeolite. Its decrease with increasing temperatures is attributed to the thermal expansion of the adsorbed phase (Supplementary Table S17). The maximum uptakes at reaction conditions (433 K for 3-heptanol and 2-methyl-3-hexanol and 373 K for 2-methyl-2-hexanol) correspond to ≈0.6, 0.6, and 0.7 mmol g^{-1} in MFI and ≈0.9, 1.1, and ≈1.2 mmol g^{-1} in BEA (Table 1). The ratio of alcohol molecule to hydronium ion (Alkanol/BAS) is ≈1.2–1.6 with MFI and 4.3–6.3 with BEA at 0.25 M (Table 1) under reaction conditions. The ratio of uptake of alcohol is higher in both zeolites than the hydronium ion concentration. Therefore, we determined first, that the hydronium ions are fully associated with alcohol molecules and second, that pores of BEA are enriched with more alkanol molecules relative to hydronium ions as compared to MFI pores.

Dehydration activity of hydronium ions inside zeolite pores

The reactivity of the alkanols in MFI and BEA shows that hydrated hydronium ions in the constrained environment were more than an order of magnitude higher than unconfined hydronium ions in H_3PO_4 solution (Figure 1). While the olefin formation rates were dependent on alcohol concentrations in H_3PO_4 solution (Figure S6 and S7), the zeolites exhibit a near zero-order rate dependence in the concentration range of ≈0.10–0.50 M, (Figure S8) driven by the complete association of hydronium ions with alkanols inside zeolite pores (Table 1). Mass transfer limitations can be ruled out based on the previous work on the zeolites for similarly-sized substrates.[5c,d] The role of pore diffusion on the kinetic measurements was further ruled out by the near-zero-order dependence of dehydration rates on alcohol concentration (Section S.2.3).

For the dehydration of 3-heptanol and 2-methyl-3-hexanol, the activation barriers on BEA resemble those in aqueous solution (Figure 1) with values 163 ± 4 and 156 ± 2 kJ mol^{-1}, respectively. The activation barriers on MFI are lower with values 143 ± 6 and 141 ± 4 kJ mol^{-1}, respectively. For both substrates, hydronium ions in the smaller pores of MFI were more reactive than hydronium ions in BEA. MFI was marginally more reactive than BEA for 2-methyl-3-hexanol, within a factor of ≈2. For 2-methyl-2-hexanol, the apparent activation barriers were similar for both BEA (131 ± 5) and MFI (128 ± 4). Notably, the wider pore BEA was more reactive than MFI for 2-methyl-2-hexanol, which contrasts the behavior of 2-methyl-3-hexanol with a very similar molecular size. It suggests that additional factors related to the alcohol structure govern the reactivity of confined hydronium ions (vide infra).

Dehydration reaction mechanism of different alkanols

We investigated the influence of the alcohol structure on the mechanism by measuring kinetic H/D isotope effects (KIE) along with ^{16}O-^{18}O exchange experiments (Table 2). KIE values between 2.1 and 2.4, 2.4 and 3.0, and 2.6 and 3.2 were observed for 3-heptanol, 2-methyl-3-hexanol, and 2-methyl-2-hexanol, respectively, for hydronium ions in solutions and inside zeolite pores. A KIE of such magnitude implies that a C_β-H(D) bond cleavage is involved in the

Table 2: H/D KIE and ^{18}O exchange experiments.[a]

Substrate	H/D KIE			^{18}O exchange/Olefin formation		
	H_3PO_4	MFI	BEA	H_3PO_4	MFI	BEA
3-heptanol	2.1	2.3	2.1	0.5	0.3	0.6
2-methyl-3-hexanol	3.0	2.4	2.8	0.9	1.0	1.0
2-methyl-2-hexanol	3.2	2.4	2.6	4.5	3.6	3.5

[a] Extent of ^{18}O exchange from $H_2{}^{18}O$ (97% isotopic purity) into unlabeled alkanol and its conversion during dehydration (concentration: 0.25 M in $H_2{}^{18}O$). H/D KIE calculated from comparison of alkanol dehydration at a concentration of 0.05–0.10 M. Details given in the Supporting Information (Tables S12–S16).

kinetically relevant step (Section S.1.5). For brevity, in an E1 mechanism, as shown in Scheme 1, an alcohol coordinates with hydronium ions. The subsequent protonation leads to an increase in standard free energy and passes through a TS ($TS_1{}^{+}$). Next, a stepwise cleavage of C-O ($TS_2{}^{+}$) and C–H ($TS_3{}^{+}$) occurs through a stable carbenium ion intermediate. The KIE values are inconsistent with C–O bond cleavage step in E1 mechanism being rate limiting. KIEs for rehybridization of α-C from sp^3 to sp^2 is estimated to be <1.35 at temperatures greater than 80 °C for all alcohols. In turn, either an E1 mechanism with a kinetically relevant C–H bond cleavage step or an E2 mechanism with concerted C-O and C–H bond cleavage is consistent with the KIE values.

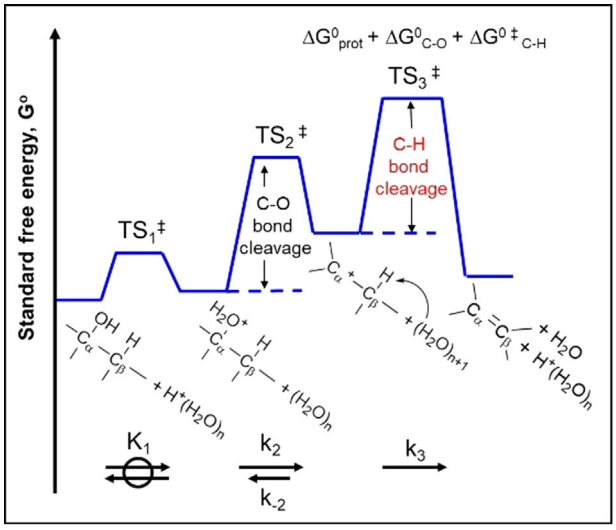

Scheme 1. Elementary steps for an E1 mechanism for alcohol dehydration to olefin in water.

The results with unlabeled alkanol and $H_2{}^{18}O$ as solvent (Table 2) at ≈0.25 M and the negligible hydration of olefin allows us to conclude that only the E1 mechanism is consistent with the large amount of ^{18}O incorporation in the recovered alcohol, whereby the ^{18}O incorporation occurs from the recombination between $H_2{}^{18}O$ and carbenium ion intermediate that follows the C–O bond cleavage (Scheme 1). The potential role of framework oxygen exchanged with ^{18}O can be ruled out,[12] as the alkanol is associated with a hydrated hydronium cluster rather than with the framework.[13] The negligible ether formation allows to rule out also the hydrolysis of formed ether as a likely pathway of ^{18}O exchange. The S_N2 pathway for ^{18}O exchange between the alkanols (secondary/tertiary) and water can be ruled out for the alkanols due to steric reasons and the reduction in local activity of water molecules in the vicinity of the protonated alcohol, involved in the S_N2 pathway.[5c,d,14]

The analysis of product selectivities further point towards an E1 elimination pathway (Section S.2.1). For example, the dehydration of 2-methyl-3-hexanol forms 2-methyl-1-hexene (formed from the C_β-H cleavage of the 2-methyl-2-hexyl carbenium ion from the 1,2 hydride shift of the 2-methyl-3-hexyl carbenium ion following C–O bond cleavage) with a selectivity of ≈15–18% on all catalysts. The largely invariant product selectivities for the alkanols in a wide range of conversion of alkanol, from ≈2–45% (Figure S10) points to the dominant coverage of alkanol-derived species on the acid site and negligible olefin hydration rates under differential conversions. The extent of ^{18}O incorporation is similar in water and in zeolite pores for all substrates, suggesting the substrate rather than the zeolite pores affect the relative relevance of C-O and C–H bond cleavage steps. The larger KIE value for 2-methyl-2-hexanol as compared to 3-heptanol is accompanied by the increased ^{18}O incorporation in the recovered alcohol. This establishes the increased relevance of C–H bond cleavage in the reaction energetics for 2-methyl-2-hexanol that follows the increased stability of carbenium ion following C–O bond cleavage step. Taken together, we conclude that all three alkanols follow E1 mechanism for the hydronium ion catalyzed dehydration on all three catalysts.

Apparent activation enthalpies ($\Delta H^{o\ddagger}$) and entropies ($\Delta S^{o\ddagger}$)

The activation enthalpies ($\Delta H^{o\ddagger}$) and entropic contributions ($T\Delta S^{o\ddagger}$) are compiled in Figure 2. It should be emphasized that both $\Delta H^{o\ddagger}$ and $\Delta S^{o\ddagger}$ include all the changes in enthalpy and entropy from the ground state to the C_β–H bond cleavage transition state ($TS_3{}^{+}$, Scheme 1), including protonation, C–O bond cleavage, and C–H bond cleavage steps. The intrinsic catalytic activity of hydronium ions is the lowest in unconstrained environments as seen by the highest $\Delta G^{o\ddagger}$ values (Supplementary Table S11). The high $\Delta S^{o\ddagger}$ on all catalysts point to a significant product-like TS with significant C_β–H bond breakage in the kinetically relevant TS for all substrates and the existence of E1 mechanism. The values of $\Delta S^{o\ddagger}$ are dependent on the microenvironment (either in unconstrained water or in zeolite pores). Notably, inside both BEA and MFI pores, the entropic contributions ($T\Delta S^{o\ddagger}$) at 400 K are within ≈4 kJ mol^{-1} for all alkanols. In general, the gain in entropy going from ground state to the TS is significantly greater in BEA compared to MFI for all the three substrates (Figure 2), attributed to the higher accessible volume inside the larger void space inside BEA pores. For an

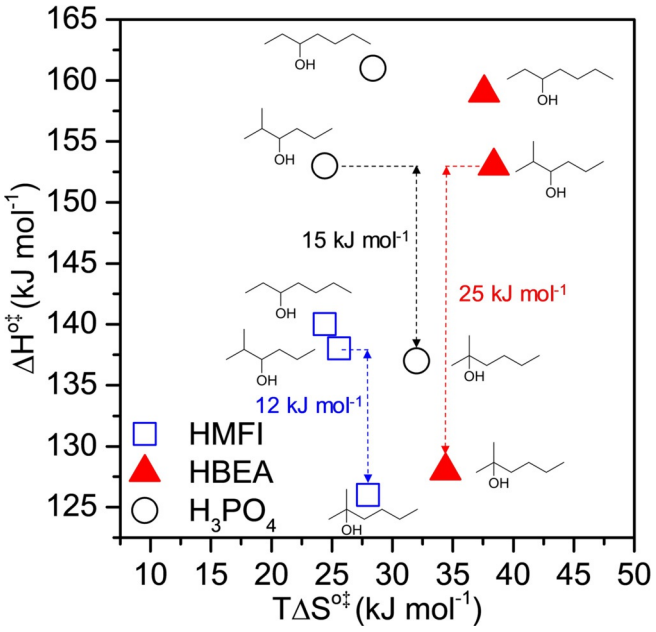

Figure 2. Activation enthalpies ($\Delta H^{o\ddagger}$) and entropic components ($T\Delta S^{o\ddagger}$) at $T = 400$ K for the hydronium ion catalyzed dehydration of 3-heptanol, 2-methyl-3-hexanol, and 2-methyl-2-hexanol in water (H_3PO_4) and MFI and BEA zeolites. Data for H_3PO_4, MFI, and BEA are shown in black, blue, and red, respectively. The activation enthalpies and entropies are derived from kinetic measurements and the TS formalism (Section S.1.4).

E1 mechanism, the similar compiled activation entropies ($\Delta S^{o\ddagger}$) for the TS of the three substrates in individual microenvironment (inside the confinements of MFI and BEA, and in solution), implies a similar activation volume compared to the ground state for the substrates in the individual microenvironments. As a note in passing, we would like to point to the two apparent compensation correlations (the two secondary alkanols and 2-methyl-2-hexanol) between standard transition enthalpies and entropies in Figure S13 with alkanol molecules in the liquid state as a reference.

We next explore the $\Delta H^{o\ddagger}$ values across the alkanols to interrogate the reactivity differences inside zeolites. There is a decrease in $\Delta H^{o\ddagger}$ from 3-heptanol to 2-methyl-2-hexanol for all catalysts, as carbenium ions after C–O bond cleavage in an E1-type pathway become more stable going from 3-heptanol and 2-methyl-3-hexanol to 2-methyl-2-hexanol, in accordance with the expected Polanyi relation for this step. With the increasing stability of the carbenium ion following C–O bond cleavage, the C_β–H bond cleavage step has a higher degree of rate control in the reaction kinetics (Table 2).

However, the impact of carbenium ion stability on $\Delta H^{o\ddagger}$ is much different over the zeolites, with the alkanol structure having a greater effect on $\Delta H^{o\ddagger}$ inside the BEA pore compared to MFI. For instance, from 2-methyl-3-hexanol to 2-methyl-2-hexanol, the activation enthalpies ($\Delta H^{o\ddagger}$) decreased by 25 kJ mol^{-1} on BEA as compared to 12 kJ mol^{-1} on MFI (Figure 2). In other words, 2-methyl-2-hexanol behaves differently in response the change of confinement dimension as compared to the two secondary alkanols. Such difference cannot be simply explained by the stability of the carbenium ion, because, if it were the dominant factor governing its activity inside the zeolite pores, the relative reactivity trends across the alkanols on zeolites should be unaffected. Next, we explore the underlying reasons for this observation and consider the different enthalpic stabilization of the C_β-H cleavage TS on BEA and MFI across the alkanols due to intraporous alkanol concentration, structural factors of the alkanols, and confinement size dimensions.

Influence of confinement dimension, intraporous alkanol concentration, and alkanol structure on enthalpic stabilization of C_β-H transition state

The activation enthalpy determines the reactivity difference among the alkanols and also their different responses to the changing confinement dimensions (provided by BEA and MFI). We first rule out the role of the nature of the ground state for the alkanols (alcohol adsorbed inside zeolite pores with hydronium ions) and the size of hydronium ion clusters. The formation of ground-state from the alkanol in the aqueous phase involves the adsorption of alkanol inside the zeolite pores and subsequent association with the hydronium ions. As noted earlier, we hypothesize the size of hydronium ion clusters inside BEA to be larger than 8 ± 1 H_2O/BAS reported inside MFI pores.[10] The favorable enthalpic or entropic contributions towards stabilization of the ground-state (inside MFI pores than BEA and across all substrates) can be ruled out via adsorption isotherms (Table 1 and Supplementary Table S22). First, only minor changes are observed in the ground-state enthalpies relative to alcohol molecules in the aqueous phase (Table 1); the differences are within 5 kJ mol^{-1} on MFI and 2 kJ mol^{-1} on BEA for all three substrates. Therefore, the changes in the $\Delta H^{o\ddagger}$ values cannot be attributed to the changes in ground-state energies relative to the TS (Supplementary Table S22). The hydronium ion protonates the associated alkanol (Scheme 1). The role of the hypothesized size difference of hydronium ion towards the stabilization of kinetically relevant C_β–H bond cleavage (and the formation of hydronium ions) inside MFI and BEA pores can be ruled out as the proton affinities of the hydronium ion cluster above five water molecules inside zeolite pores has been suggested to be negligible.[5c,d]

$$\Delta H^{o\ddagger}_{\text{Zeolite}} = \Delta H^{o}_{\text{Des alcohol}} + \Delta H^{o}_{\text{Deprotonation H+(H}_2\text{O)}n} + \Delta H^{o}_{\text{Des (H}_2\text{O)}n} + \Delta H^{o}_{\text{DPE}} + \Delta H^{o}_{\text{Protonation (H}_2\text{O)}n} + \Delta H^{o\ddagger}_{\text{Homogenous}} - \Delta H^{o}_{Es} - \Delta H^{o}_{\text{vdW pore}} - \Delta H^{o}_{\text{Intermolecular Alcohol}} \quad (1)$$

We consider next the differences in enthalpic stabilization of the C_β–H bond cleavage due to differences in the intraporous alkanol concentration, structural factors of the alkanols, and confinement size dimensions that govern the difference in the observed trends in reactivity for MFI and

BEA across the alkanols. Besides a larger confinement provided by BEA, the ratio of alcohol molecule to hydronium ion is 4.3–6.3 inside BEA pores, which is much larger than ≈1.2–1.6 with MFI at 0.25 M under reaction conditions (Table 1). It suggests there exists at most one alcohol molecule between hydronium clusters on MFI and at least five for 2-methyl-2-hexanol vs. three and four for 3-heptanol and 2-methyl-3-hexanol, respectively, assuming association of one alcohol molecule with each hydronium ion. We note that the BEA pores were enriched with 2-methyl-2-hexanol as compared to other alkanols (Table 1), which is hypothesized to be caused either by the steric factors or by more favorable interactions of 2-methyl-2-hexanol with defect sites on BEA (internal silanol groups, Figure S1) as compared to water. Such enrichment of alkanols in the pore is likely to play an important role for stabilizing TS via intraporous intermolecular interactions.

We now first examine the difference between BEA and MFI in the enthalpic stabilization of the C_β-H TS over a given alkanol by analyzing a Born-Haber thermochemical cycle and then elucidate how structural differences of these alkanols further impact the reactivity differences between the two zeolites. As shown in Scheme 2, analysis of such a thermochemical cycle helps in the investigation of how zeolite pores and alcohol properties individually influence the observed activation enthalpy.[3] The considered steps are arbitrary, but the state function nature of thermodynamics enables the decoupling the catalyst and molecular effects.[3]

The thermochemical cycle includes steps such as 1) desorption of an alcohol molecule to the liquid (water) phase; 2) deprotonation of the hydrated hydronium ion leading to a "dry" proton on the framework Al and water cluster and 3) desorption of water cluster into the liquid phase; 4) deprotonation of the "dry" proton and moving the proton to non-interacting distances (deprotonation energy); 5) protonation of water cluster to form hydrated hydronium ion in aqueous phase; 6) protonation of alcohol, C–O bond cleavage of the alcohol in the liquid phase leading to the relevant late C_β–H bond cleavage TS (as shown in Scheme 1). The final step for placing the TS inside the zeolite pore can be further considered to be composed of 7) an electrostatic component given by the interaction of the TS with the negative charge on the framework, 8) the van der Waals (vdW) interactions of the TS with the pore walls, and 9) intraporous intermolecular interactions considering there exists more than one alkanols near TS in the zeolite pores. The thermochemical cycle enables representation of the activation enthalpy of late C_β–H bond cleavage TS with respect to the steps (1) through (9).

We first consider that step 2, 4, 5, 6, and 7 are expected to be similar for MFI and BEA. The deprotonation energy of dry proton (step 4), which is independent of the confinement as interaction of zeolite pores and protons are not appreciably affected by the confinement.[15] The electrostatic component (step 7) would depend on the charge distribution in the TS and their interaction with the anion. Such charge distributions can be considered to be similar across all zeolite frameworks because of similar acid strengths and similar stabilities of conjugate anions at all framework locations.[15]

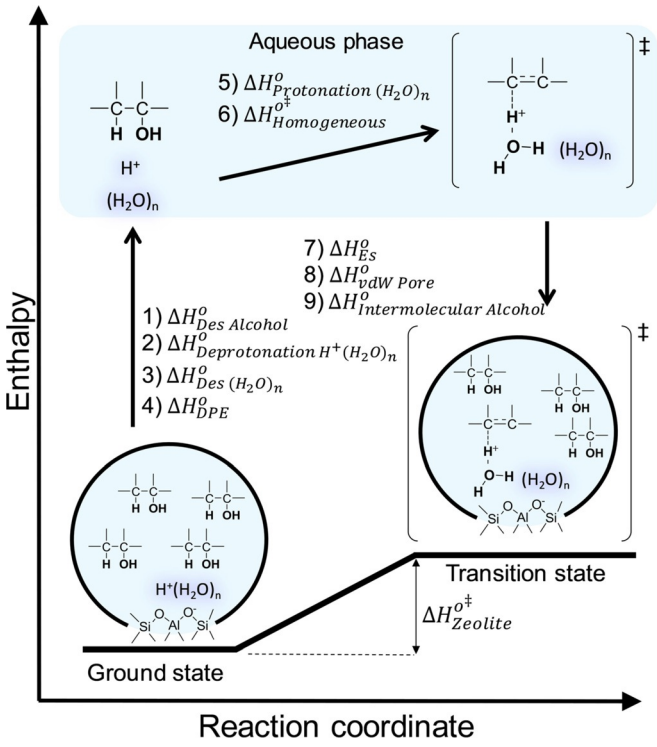

Scheme 2. Thermochemical cycle for the elimination transition state of alkanols inside zeolite pores. The thermochemical cycle involves the formation of the C_β-H TS ($\Delta H^{o\ddagger}_{Zeolite}$) inside zeolite pores from the ground state (alcohol adsorbed inside zeolite pores). The TS formation has contributions from the desorption of reacting alcohol ($\Delta H^o_{Des\ Alcohol}$), deprotonation of the water cluster ($\Delta H^o_{Deprotonation\ H+(H_2O)n}$), desorption of the water cluster ($\Delta H^o_{Des\ (H_2O)n}$), and deprotonation enthalpy (ΔH^o_{DPE}) to non-interacting distances in the aqueous phase. This is followed by protonation of water cluster to form hydronium ions ($\Delta H^o_{Protonation\ (H_2O)n}$) and subsequent formation of C_β-H TS ($\Delta H^{o\ddagger}_{Homogeneous}$) in aqueous phase. Finally, the C_β-H TS is adsorbed back inside the zeolite pores with contributions from electrostatic interaction of the ion-pair (ΔH^o_{Es}), the van der Waals stabilization from the zeolite pore walls ($\Delta H^o_{vdW\ Pore}$) and the intermolecular interactions with intraporous alkanol molecules ($\Delta H^o_{Intermolecular\ Alcohol}$).

In contrast, the deprotonation (step 2) and protonation energies (step 5) may be considered to be slightly different across zeolites due to varying hydronium ion cluster size. However, proton affinities of hydronium-ion size clusters start approaching a constant value as the cluster size starts approaching a size of $n = 5$, as compared to a size larger than 8 ± 1 inside MFI and BEA pores.[5c] Therefore, the enthalpic values of steps 2 and 5 are not expected to vary appreciably. Step 6, hydronium-ion catalyzed dehydration in water without zeolite confinement, leading up to the TS is also independent of the zeolites.

Therefore, the activation enthalpy difference between MFI and BEA for a given alkanol, $\Delta\Delta H^{o\ddagger}_{MFI\text{-}BEA}$ is given by:

$$\Delta\Delta H^{o\ddagger}_{MFI-BEA} = \Delta\Delta H^{o}_{Des\ Alcohol,\ MFI-BEA} + \Delta H^{o}_{Des\ (H2O)n,\ MFI-BEA} - \left(\Delta\Delta H^{o}_{vdW,MFI-BEA} + \Delta\Delta H^{o}_{Intermolecular\ Alcohol,\ MFI-BEA}\right) \quad (2)$$

The contribution from desorption of alcohol (step 1) can be estimated by adsorption enthalpies calculated from the isotherms (Table S21). Together with the measured activation enthalpy, the combined vdW (step 8) and intermolecular interactions (step 9) along with the desorption of water cluster (step 3) contributing towards the difference in stabilization of TS in BEA pores compared to MFI is estimated to be 25, 20, and 5 $kJ\,mol^{-1}$ for 3-heptanol, 2-methyl-3-hexanol, and 2-methyl-2-hexanol, respectively. The desorption enthalpies of water cluster are not expected to be alkanol-structure dependent, but rather dependent on the zeolite pore. We infer, therefore, the pore environment inside the BEA pore, which enables the combined vdW and intermolecular interactions accounts for the higher enthalpic penalties in the formation of the TS going from 2-methyl-2-hexanol to 3-heptanol.

The question arises now as to how structural differences of the alkanols, especially between the tertiary 2-methyl-2-hexanol and the secondary 2-methyl-3 hexanol and 3-heptanol, impact the vdW interaction of TS with zeolite pore and the intraporous intermolecular interactions differently in MFI and BEA. On one hand, with the decreasingly enthalpically demanding TS formation from 3-heptanol to 2-methyl-2-hexanol (Figure 2), the vdW stabilization provided by the narrower MFI pore over BEA assumes reduced significance from the secondary to tertiary alkanols. On the other hand, with the increasing ease of TS formation, the intraporous stabilization provided by the co-adsorbed alkanol molecules inside BEA assumes greater significance than the weaker vdW stabilization, making BEA more reactive. As BEA is entrained with more alkanol molecules than MFI, these intermolecular interactions assume greater significance. Bregante et al. have reported enthalpically unfavorable interactions between long aliphatic chain of olefin epoxidation TS with water clusters.[7] Therefore, the higher entrainment of alkanol molecules in BEA pores increases the relative importance of TS-alkanol interactions than TS-water interactions. The increased stabilization of TS of 2-methyl-2-hexanol as compared to secondary alcohols inside BEA pores relative to MFI may be attributed to this larger enthalpic stabilization driven by favorable TS-intraporous alkanol interactions. While the role of alkanol structure on the enthalpic stabilization of C_β-H TS is clear from our data, the defect sites and pore hydrophilicity can also contribute to the differences in alkanol uptakes inside zeolite pores and the stabilization of C_β-H TS.[7,16] This can be further explored with zeolites with different Si:Al ratio and different synthesis methods.[7,16] Despite the difficulty in deconvolution of the number of such complex interactions that affect the reactivity on a solid–liquid interface, our study provides an important step in furthering the understanding of the catalysis at solid–liquid interfaces.

Conclusion

We show here how the steric constraints of zeolite pores influence the catalytic activity of hydronium ions and how the environment influences the local organization of solvents and substrate molecules. The higher dehydration rates of secondary alkanols, 3-heptanol and 2-methyl-3-hexanol, in MFI zeolite with pores smaller than those of zeolite BEA, is caused by a lower activation enthalpy in the tighter confines of MFI. It offsets a less positive activation entropy. With the increasing ease in the formation of C_β–H TS for 2-methyl-2-hexanol, the stabilization provided by the confinement assumes lesser significance and an additional enthalpic stabilization of the TS due to dispersive interactions with other alcohol molecules become important. This makes the larger-pore BEA zeolite more reactive than the smaller-pore MFI zeolite for dehydration of 2-methyl-2-hexanol. Our results demonstrate additional avenues for tuning the microenvironment inside the zeolites to enhance rate kinetics inside nanoscopic confinements.

Acknowledgements

This work was part of the Chemical Transformations Initiative at the Pacific Northwest National Laboratory (PNNL), conducted under the Laboratory Directed Research and Development Program at PNNL. D.M.C. and J.A.L. were supported by the U.S. Department of Energy (DOE), Office of Science, Office of Basic Energy Sciences, Division of Chemical Sciences, Geosciences and Biosciences (Transdisciplinary Approaches to Realize Novel Catalytic Pathways to Energy Carriers, FWP 47319) for contributing to the discussion of the results, planning, and writing of the manuscript. Some of the experiments were performed at the William R. Environmental Molecular Science Laboratory, a national scientific user facility sponsored by the DOE Office of Biological and Environmental Research located at Pacific Northwest National Laboratory. Open access funding enabled and organized by Projekt DEAL.

Conflict of interest

The authors declare no conflict of interest.

Keywords: aliphatic alcohols · confinement effect · enthalpy-entropy compensation · hydronium ion · zeolites

[1] a) S. H. Chai, H. P. Wang, Y. Liang, B. Q. Xu, *Green Chem.* **2007**, *9*, 1130; b) R. Weingarten, J. Cho, W. C. Conner, G. W. Huber, *Green Chem.* **2010**, *12*, 1423; c) P. A. Zapata, J. Faria, M. P. Ruiz, R. E. Jentoft, D. E. Resasco, *J. Am. Chem. Soc.* **2012**, *134*, 8570; d) C. Zhao, J. A. Lercher, *Angew. Chem. Int. Ed.* **2012**, *51*, 5935; *Angew. Chem.* **2012**, *124*, 6037.

[2] a) P. Deshlahra, R. T. Carr, E. Iglesia, *J. Am. Chem. Soc.* **2014**, *136*, 15229; b) P. Deshlahra, E. Iglesia, *J. Phys. Chem. C* **2016**, *120*, 16741; c) L. Annamalai, Y. L. Liu, S. Ezenwa, Y. L. Dang, S. L. Suib, P. Deshlahra, *ACS Catal.* **2018**, *8*, 7051.

[3] G. Noh, Z. C. Shi, S. I. Zones, E. Iglesia, *J. Catal.* **2018**, *368*, 389.

[4] P. Deshlahra, E. Iglesia, *ACS Catal.* **2016**, *6*, 5386.

[5] a) Y. S. Liu, E. Barath, H. Shi, J. Z. Hu, D. M. Camaioni, J. A. Lercher, *Nat. Catal.* **2018**, *1*, 141; b) S. Prodinger, H. Shi, H. M. Wang, M. A. Derewinski, J. A. Lercher, *Appl. Catal. B* **2018**, *237*, 996; c) Y. S. Liu, A. Vjunov, H. Shi, S. Eckstein, D. M. Camaioni,

D. H. Mei, E. Barath, J. A. Lercher, *Nat. Commun.* **2017**, *8*, 14113; d) H. Shi, S. Eckstein, A. Vjunov, D. M. Camaioni, J. A. Lercher, *Nat. Commun.* **2017**, *8*, 15442.
[6] M. A. Mellmer, C. Sener, J. M. R. Gallo, J. S. Luterbacher, D. M. Alonso, J. A. Dumesic, *Angew. Chem. Int. Ed.* **2014**, *53*, 11872; *Angew. Chem.* **2014**, *126*, 12066.
[7] D. T. Bregante, A. M. Johnson, A. Y. Patel, E. Z. Ayla, M. J. Cordon, B. C. Bukowski, J. Greeley, R. Gounder, D. W. Flaherty, *J. Am. Chem. Soc.* **2019**, *141*, 7302.
[8] R. Gounder, *Catal. Sci. Technol.* **2014**, *4*, 2877.
[9] J. Rorrer, S. Pindi, F. D. Toste, A. T. Bell, *ChemSusChem* **2018**, *11*, 3104.
[10] S. Eckstein, P. H. Hintermeier, R. X. Zhao, E. Barath, H. Shi, Y. Liu, J. A. Lercher, *Angew. Chem. Int. Ed.* **2019**, *58*, 3450; *Angew. Chem.* **2019**, *131*, 3488.
[11] a) F. Eder, J. A. Lercher, *J. Phys. Chem. B* **1997**, *101*, 1273; b) F. Eder, J. A. Lercher, *Zeolites* **1997**, *18*, 75.
[12] S. M. Pugh, P. A. Wright, D. J. Law, N. Thompson, S. E. Ashbrook, *J. Am. Chem. Soc.* **2020**, *142*, 900.
[13] D. H. Mei, O. A. Lercher, *J. Phys. Chem. C* **2019**, *123*, 25255.
[14] C. A. Bunton, A. Konasiewicz, D. R. Llewellyn, *J. Chem. Soc.* **1955**, 604.
[15] L. Qi, R. Alamillo, W. A. Elliott, A. Andersen, D. W. Hoyt, E. D. Walter, K. S. Han, N. M. Washton, R. M. Rioux, J. A. Dumesic, S. L. Scott, *ACS Catal.* **2017**, *7*, 3489.
[16] M. J. Cordon, J. W. Harris, J. C. Vega-Vila, J. S. Bates, S. Kaur, M. Gupta, M. E. Witzke, E. C. Wegener, J. T. Miller, D. W. Flaherty, D. D. Hibbitts, R. Gounder, *J. Am. Chem. Soc.* **2018**, *140*, 14244.

Manuscript received: July 17, 2020
Accepted manuscript online: October 2, 2020
Version of record online: November 27, 2020

